BMC Plant Biology

RESEARCH Open Access

Postharvest detection of anthracnose (*Colletotrichum asianum*) on mango fruit (*Mangifera indica* L. cv Namdokmai Sithong) using near-infrared response

Apiwat Junto[1], Thitima Phanomsophon[2], Sneha Sharma[3], Kannapot Kaewsorn[1], Jiraporn Sripinyowanich Jongyingcharoen[4], Cheewanun Dachoupakan Sirisomboon[5*], Panan Rerngsamran[5], Panmanas Sirisomboon[4*], Pimpen Pornchaloempong[6], Norhashila Hashim[7,8], Prabhas Chongstitvatana[9] and Anupun Terdwongworakul[10]

Abstract

Anthracnose disease, caused by fungi of the genus *Colletotrichum*, poses a major threat to mango production and export industries, with *Colletotrichum asianum* being among the most significant pathogenic species. This work proposes the hypothesis that the simple difference in absorption between anthracnose-infected and noninfected mangoes illustrated by the average near-infrared (NIR) spectra obtained from hyperspectral images could be used for simple differentiation of the two groups. The method of depositing fungal spores by spraying the spores over the fruit surface, not a small area or specific point, allows for the number of spores per unit area to be harmonized and to detect infected or noninfected spores on every pixel of the mango surface using a hyperspectral imaging camera. Important wavelengths for differentiation included water bands of 970, 1190, and 1200 nm which resulted in the greatest difference in absorbance, and bands of chitin, the major component of the fungal cell wall; 1195 nm was the most important band. In addition, the vibration bands of 868 (protein in the fungal cell wall), 1134 (sugar and starch of the mango substrate), 1320 (NIR absorbers in the fungus-sprayed and mango substrate, not specifically defined) and 1069 nm (crystallinity and N-acetyl methyl groups in the fungal chitin and constituents of the mango), differed from each other. These wavelengths can be used for modelling, which can lead to high performance in quantifying the concentration of anthracnose and classifying the strength levels of anthracnose infection. The microbiological mechanism of anthracnose growth on infected mangoes corresponding to changes in the NIR spectrum during the 4 days after spore infection is comprehensively discussed. These results can aid in enhancing early detection and classification techniques for anthracnose-infected mangoes from noninfected mangoes using hyperspectral image sensors.

*Correspondence:
Cheewanun Dachoupakan Sirisomboon
cheewanun.d@chula.ac.th
Panmanas Sirisomboon
panmanas.si@kmitl.ac.th

Full list of author information is available at the end of the article

Keywords Near-infrared spectrum, Postharvest, Hyperspectral imaging, Anthracnose, Fungus, Mango

Introduction

Mango (*Mangifera indica* L.) is a famous fruit of Thailand and has export potential. There are many varieties of export quality mangoes, but the most popular is *"Mangifera indica* L. cv Namdokmai Sithong" [1] because of its aroma, which is rich in nutrients and phytonutrients (e.g., vitamin C, vitamin E, beta-carotene, lutein, quercetin, mangiferin, omega 3, omega 6, and polyunsaturated fatty acids) [2]. The Trade Policy and Strategic Office (TPSO), Ministry of Commerce, Thailand [3], reported that Thailand exports mangoes to its major trading partners; South Korea as the largest importer, with 83,211,090 USD (2,931 million Baht) in 2024, which is an expansion of 132.7% compared with that in 2023, and Malaysia as the 2nd largest importer.

Anthracnose disease caused by *Colletotrichum* spp. is a major problem for fresh mango industries in terms of exports and production [4]. Under hot and humid weather, the yield loss caused by anthracnose increases [5]. Although the fungus can reproduce and destroy plants at any stage of mango growth, the primary concern is the fruits, as the signs of the disease are not visible in an infected unripe mango but become visible during fruit ripening [6].

Infection occurs when the conidia of the fungus land on the fruit surface, develop appressoria that penetrate the cuticle, and the hyphae infiltrate the flesh. Small black round or irregular spots appear and later enlarge as the mango ripens, followed by softening and rotting [5, 7]. An infected mango caused by anthracnose is shown in Fig. 1. At present, there are no varieties of mango that can completely tolerate or be protected from anthracnose. Therefore, it is necessary to use chemicals to prevent and inhibit the growth of anthracnose and other mould diseases [5]. These chemicals directly impact and damage the environment and increase the cost of mango production. It is necessary to find other ways to prevent the disease and maintain the quality the of mangoes. Among these options, the use of essential oils from certain plants as inhibitors to arrest the growth of fungi during postharvest storage has been reported [8, 9]. A combination of hot water and UV-C radiation treatment has been suggested as a tool for preventing infection and inhibiting anthracnose [10]. The methods mentioned above are used for extending the period to maintain quality and prevent disease in mangoes, which yield favourable outcomes. However, this does not guarantee good-quality mangoes that are devoid of anthracnose for exporters and consumers. Therefore, early detection methods for pathogens such as *Colletotrichum* infection in mango fruits are necessary.

The near-infrared spectroscopy (NIRS) technique, which uses shorter IR wavelengths (800–2500 nm) than the mid-infrared range (MIR) (2500–15000 nm) [11], has recently been employed for the early detection of anthracnose on fruits such as olive [12], Kent mango [13], and Namdokmai Sithong mango [14]. The application of neural networks for the early detection of anthracnose in olives using near-infrared (NIR) hyperspectral images revealed that olive fruit infection could be detected 3 days after exposure at 85 to 100% accuracy [12]. Detection of anthracnose in Kent mango fruits using Vis–NIR hyperspectral imaging by the quadratic discriminant analysis (QDA) model showed remarkable performance for anthracnose detection using multiple classifications and with an accuracy of no less than 80% [13]. By inoculating 20 µl of a 1×10^6 spore/ml suspension of *Colletotrichum gloeosporioides* onto the fruit, Sonthiya [14] reported the use of NIRS to detect anthracnose in 'Namdokmai Sithong' mangoes. The mangoes were then placed in a box at 28 °C and 100% relative humidity for 24 h. The inoculated area was subsequently scanned for early detection using a contacting fibre optic probe in the range of 800–2500 nm. The noninfected peel, obtained by cleaning with distilled water and air-drying at room temperature, was located on the opposite side of the infected mango. NIR spectrum analysis using partial least squares discriminant analysis (PLS-DA) revealed that the standard normal variate (SNV)-modified spectrum could distinguish between mangoes with anthracnose fungi and the control with an accuracy of 95.1%, and the important wavelengths for classification were 1152, 1725, and 1880 nm, as determined by the high regression coefficients.

Thus, a detection technique using differences in absorption between noninfected and anthracnose-infected mangoes, as illustrated by the average near-infrared spectra obtained from hyperspectral images, could be used as a simple method to differentiate the two groups of mangoes.

Materials and methods

Collection of fruit samples

Thirty seemingly healthy (n = 30) mango fruits from Namdokmai Sithong were collected from a plantation (Ban Tha Thong Mango Community Enterprise, Doem Bang Nang Buat District, Suphan Buri Province, Thailand 13.69167° N, 99.93000° E) and used in this experiment. Fruits were selected according to the export benchmarks of the Thai Agricultural Standard: TAS-5–2024-Mango [15], and mango fruits were collected on the basis of the commercial maturity index at 90 days after fruit bud initiation [16]. The collected fruits were uniform in size,

Fig. 1 Anthracnose lesions on mango

shape, and skin tone and lacked defects or disease incidence. All mango fruits were harvested on 20 April 2023. Out of 30 fruits, 29 fruits were used in the experiment because one fruit showed no infection for analysis of different absorption spectra of control (noninfected) and infected mangoes.

In addition, the changes in the NIR spectra of the treated mangoes during the 4 days after spore deposition corresponded to the infection mechanism of anthracnose growth on the mangoes, which was observed using another set of samples (210 mango fruits, cv. Namdokmai Sithong). These fruits were collected from six mango plantations in Thailand's central plains, consisting of three orchards, namely, Rachaen Farm, Bang Phae District, Ratchaburi Province 13.69167°N, 99.93000°E (16 Feb 2023), Rachaen Farm, Pak Tho District, Ratchaburi Province, 13.36833°N, 99.83000°E (20 Feb 2023), and Ban Tha Thong Mango Community Enterprise, Doem Bang Nang Buat District, Suphan Buri Province, 14.85361°N, 100.09778°E (20 Apr 2023), and the eastern region of another three orchards, Kiat Umporn Mango Orchard, Phanom Sarakham District, Chachoengsao Province, 13.74444°N, 101.34694°E (26 Apr 2023), Kaew Wongnukul Orchard, Wang Sombun District, Sa Kaeo Province, 13.35150°N, 102.18333°E (30 Apr 2023), and Kaew Wongnukul Orchard, Wang Nam Yen District, Sa Kaeo Province, 13.51094°N, 102.17471°E (2 May 2023), where mango is widely cultivated for export. In the sample collection, 30 mangoes were obtained from each orchard, with 1–5 mango fruits per tree and 10 mango trees per plantation.

Fungal spore preparation

Colletotrichum asianum previously isolated and purified from diseased mango fruit using a single-spore isolation technique [17] was used in this study. Pathogenicity testing confirmed that the fungal isolate caused anthracnose symptoms in mango. The isolate was identified on the basis of morphological and ITS sequencing, and its identity as *Colletotrichum asianum* was established. A spore suspension of *C. asianum*, which was previously isolated from diseased mango, was spread onto PDA plates and incubated at room temperature under a 12-h light/dark cycle until full sporulation occurred, typically within 7–10 days. Sterile distilled water (5–10 ml) was added to the fully sporulated plates, and the spores were harvested by gently scraping them using a sterile inoculating loop. The spore suspension was collected into a Falcon tube, vortexed, and then filtered through sterile cheesecloth to collect the spore suspension. Spores were counted and adjusted to 1×10^5 conidia/ml using a haemocytometer.

Preparation of fruit samples with different spore intensities for near-infrared hyperspectral imaging (NIR-HSI)

Fungal spores were deposited onto the mango fruit surface using a simulated natural method, in which a spore suspension was sprayed, allowing them to penetrate beneath the peel without mechanical aid. A Mini Airbrush Compressor (AS176; China) was used to spray the fungal spore suspension onto mango fruits to achieve uniform deposition.

The mango fruits of the cultivar Namdokmai Sithong were sterilized by soaking in a water bath at 55 °C for 5 min as previously described [18], then soaked in sterile cold water for 5 min, and left to dry in a laminar flow; then, the fruits were grouped into five (n = 5) treatment sets, with each set containing 6 mango fruits (2 for control and 4 for treatments). The 2 control fruits were sprayed only with sterile distilled water, while the 4 treatment fruits were sprayed with a fungal spore suspension. To simulate different spore inoculum levels, the fruits in sets 1–5 were sprayed with fungal spore suspension (4 × 5 = 20 fruits) or sterile water (control fruits) for 1, 2, 3, 4, and 5 rounds (2 × 5 = 10 fruits), respectively. In addition, to validate spore viability, a parallel experiment was conducted on PDA plates. Treatment plates were sprayed with the fungal spore suspension, and control plates were sprayed with sterile water; 1, 2, 3, 4, and 5 spray rounds were applied to each respective set. All the applications were performed in triplicate. The plates were then incubated, and the number of colony-forming units (CFUs) was determined using a digital colony counter. The sprayed mangoes were stored in translucent plastic boxes

at an air-conditioned temperature of 25 °C with 67% relative humidity (average conditions in Thailand) for 10 days. This condition allowed for the mangoes to ripen, after which the occurrence of anthracnose disease on the mangoes was observed.

Hyperspectral imaging system and image acquisition

Hyperspectral images of the fruit samples were obtained daily for 8 days from the date of spraying with fungal spores (DAY 00) until DAY 08. A total of 10 control fruits with 5 different numbers of rounds of sterile water spraying were scanned for 8 days, and a total of 20 infected fruits with 5 different numbers of rounds of 5 levels of spores per cm^2 sprayed (7.08, 9.60, 12.30, 12.59, and 13.33 spores/cm^2) were scanned. The hyperspectral acquisition systems (Fig. 2) included a push broom NIR-HSI configuration system with a linear array of 320 CCD detectors (Xeva 992, Xenics Infrared Solutions, Belgium) and an imaging spectrograph (Imspector N17E Specim, Spectral Imaging Ltd., Oulu, Finland) with an 800–1700 nm and 3.2-nm resolution sensor detector. The system was composed of two tungsten-halogen light sources (Lowel Light Inc., New York, USA) of 500 Watts, adjusted at an angle of 45°, to deliver uniform lighting in the field of view, and the sample in a transparent plastic box without a lid was subjected to HSI on the translation stage and scanned at a stage speed of 10 ms^{-1}. The white and dark references for background compensation were concurrently acquired with the NIR-HSI images for radiometric correction. A Spectralon® reflectance material with a relative reflectance of 99% was used to capture the white reference, and the dark reference was automatically acquired by the NIR-HSI system by closing the camera shutter. The system operation was controlled by a computer with Specim's LUMO Software Suite (Spectral Imaging Ltd., Oulu, Finland). The distance between the camera lens and the top surface of the mango was approximately 30 cm, with a spatial resolution of 30 µm per pixel and an optimized integration time of 9 ms. After image acquisition, the raw hypercube was normalized using Eq. (1) to eliminate the instant noise due to the scanning background and the electronic drift of the detector.

$$R = \frac{R_s - R_d}{R_w - R_d} \quad (1)$$

where R is the relative reflectance image, R_s is the raw reflectance image, R_d is the dark reference image, and R_w is the white reference image.

Extraction of the region of interest

NIR absorption information is collected from the hyperspectral images of the samples in the form of images. As a result, normalized NIR spectral data are required to remove physical phenomena in the spectra and to improve the performance of an algorithmic model. Specifically, a subset of an image was selected to identify the region of interest (RoI) and exclude confounding regions. An NIR-HSI image prior to RoI extraction, consisting of a mango fruit, background, transparent plastic container, shadows, and moist cotton ball, is shown in Fig. 3(A). This study was conducted using the method described by Tsai and Guan [19] with minor modifications to isolate the area of interest (i.e., mango fruit) from other regions (background, plastic container, shadows, and cotton balls). The mango fruits were identified by RGB colour and wavelengths of 970 nm related to H_2O and 1440 nm related to sucrose [20], and Fig. 3(B) shows the RoI-extracted image of the mango fruit.

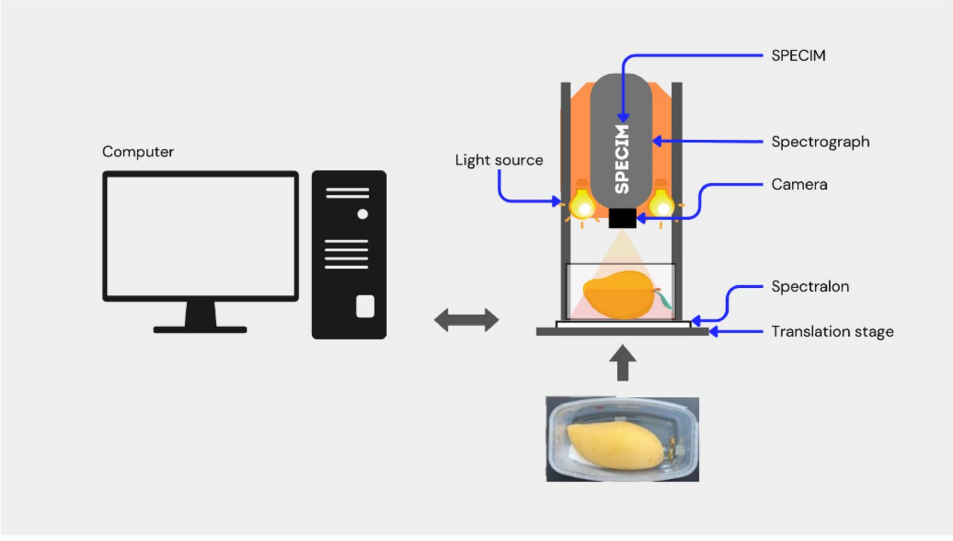

Fig. 2 Experimental setup of the push broom NIR-HSI system

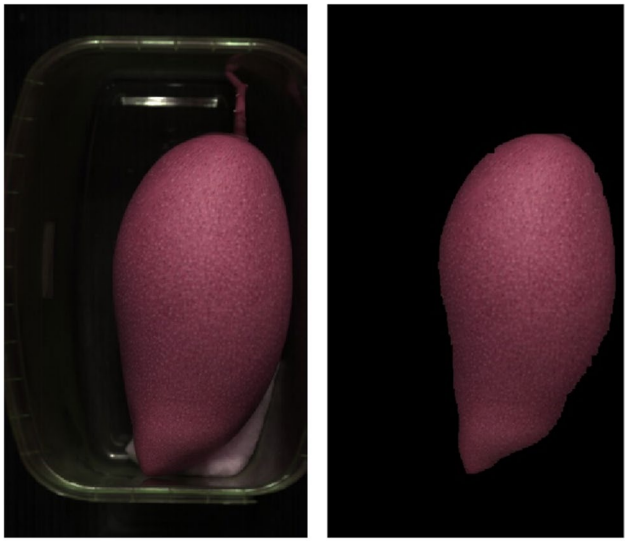

Fig. 3 **A** NIR-HSI image and **B** RoI-extracted image of mango fruit

Spectral analysis of the difference in absorbance between control and infected spectra of fruits

The average original spectra from every pixel of each image acquired on different days (DAY 00, DAY 01, DAY 02, DAY 03, DAY 04, DAY 05, DAY 06, Day 07, and DAY 08) for both control and infected samples with spore counts of 7.08, 9.60, 12.30, 12.59, and 13.33 spores/cm^2 were calculated, and the difference between the control and infected spectra at each wavelength (860–1650 nm with a resolution of 3.2 nm) was obtained by subtracting between the infected absorbance and control absorbance. The values at the water vibration bands of 970, 1190, and 1450 nm and at the chitin vibration bands of 1195, 1505, and 1583 nm were compared. In addition, the maximum difference in the absorbance was also detected. The NIR vibration bands of water and chitin and the bands corresponding to the maximum difference were analysed.

Spectral analysis of the microbiological mechanism corresponding to changes in the NIR spectrum

The average change in the spectra of 210 mango fruits in the 2nd set during the 4 days after spore infection corresponded to the microbiological mechanism of fungal growth. The spectra were pretreated by standard normal variate (SNV) for comparison without distortion by physical effects, and the spectral characteristics, especially the absorption peaks related to the biochemical constituents in *C. asianum* and the dominant peaks of major constituents or peaks of the NIR absorber in the fungus and mango substrate, were analysed.

Results and discussion

Spectral data of control and infected mango samples and its different

Hyperspectral imaging systems are an ideal method for evaluating the quality of fruit in a nondestructive manner that relies mainly on chemical properties and physical related to chemical properties. NIR wavelengths ranged from 800 to 1700 nm for 29 mango fruits, which were divided into control mangoes (10 fruits that were not infected) and infected mangoes (19 fruits). The average raw spectra of the control and infected mangoes at 0, 24, 48, 72, 96, 120, 144, 168 and 192 h postinoculation are shown in Fig. 4(A). The spectra show the sterile water-sprayed mango at 0 h, which should be the vibration of only the mango substrate, whereas the others contained the average of the five densities of *C. asianum* inoculum and progressed to fungus growth over time. The figure shows the different absorption peaks of the chitin at 1195 nm. The spectra of the sterile water-sprayed plants and *C. asianum*-sprayed plants were similar at 0 h. The averaged spectra for durations of 1–4 days (24, 48, 72 and 96 h) where no anthracnose lesions were detected, as shown in Fig. 4 (C, top), were close to the 0 h average spectra, indicating that the growth of the fungus might be slow in these stages but were obviously different from the 0 h average spectra. The higher-density spectra (120, 144, 168, and 192 h) of DAY 05–08 (Fig. 4 (C, bottom)) were farther from the 0 h average spectra, indicating more growth progress than the former group. However, the average absorbance of the infected mango samples fluctuated from 24 to 192 h, but the average spectra clearly differed from each other and at 0 h, indicating that the effects of the different matrices of the mango substrate were greater during ripening than during the growth of the fungus.

The difference in the representative spectrum of *C. asianum*-sprayed mango at 192 h between asymptomatic (no defect) and symptomatic (infected) locations is large (Fig. 4(B)). Owing to the assumption of uniform spread of *C. asianum* over the mango surface by spraying, the growth and lesion of the fungus should have been similar, but the opposite results were obtained: the lesions after 192 h showed as spotting, and the absorbance of the asymptomatic (no defect) and symptomatic (infected) locations was high, indicating that the effect of the radius of curvature of the mango fruit and the substrate under the peel on the middle line of the longitudinal axis of the fruit facilitated the growth of the fungus, as shown in Fig. 4(C).

The important wavelengths for differentiating the control (noninfected) and anthracnose fungus-infected mangoes by using different absorbances on the NIR spectra of both groups indicated that among the water bands related to changes in anthracnose on mango peels, 970

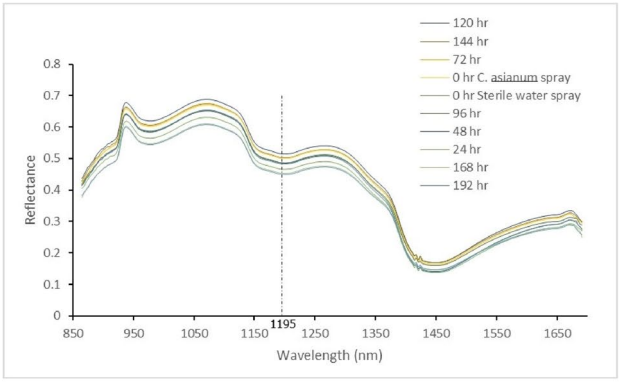

A

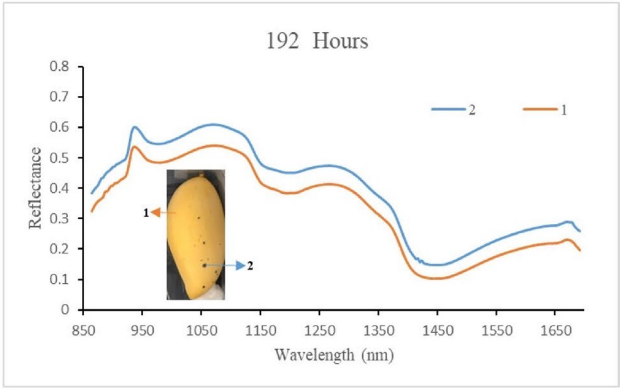

B

C

Fig. 4 Averaged NIR spectra of mango fruits. **A** Spectra measured at 0 h after sterile water was sprayed (10×9 = 90 spectra), 0 h after *C. asianum* was sprayed (19×9 = 171 spectra) and 24, 48, 72, 96, 120, 144, 168 and 192 h postinoculation. (19×8 = 152 spectra) from 10 control mangoes and 19 mangoes infected with *C. asianum* at five initial inoculum densities: 7.08, 9.60, 12.30, 12.59, and 13.33 spores/cm^2. **B** Comparison of representative spectra of *C. asianum*-sprayed mango at 192 h from asymptomatic (no defect) (#1 in the figure) and symptomatic (infected) (#2 in the figure) locations. **C** Mango fruit corresponding to the progression of anthracnose infection from 24 h to 192 h postinoculation

and 1190 or 1200 nm differed the most (Table 1). The 1450 nm band, referred to as the combined vibration of water and starch in mango, showed the least difference, indicating that the effect of the water vibration is stronger.

The 1450 nm band of the combined vibration of the ν1 O-H symmetric stretch and the ν3 O-H asymmetric stretch of the water molecule were 5 times lower than the 970 nm and 1190 nm or 1200 nm bands in a combination of 2 fundamental vibrations of symmetric stretch (2ν1) and an asymmetric stretch (ν3) of O-H bonds and a combination of symmetric stretch (ν1), bending (ν2), and asymmetric stretch (ν3) of the water molecule. These results indicate that the combination of the 3 fundamental vibrations with bending mode was stronger than the 2 fundamental combinations were.

Chitin is an essential major component of the cell walls and septa of all pathogenic fungi. Chitin is a β(1,4)-homopolymer of N-acetylglucosamine that folds in an antiparallel manner, forming intrachain hydrogen bonds [23]. Chitin chains are covalently cross-linked to β(1,3)-glucan to form the inner skeleton of most fungi [23].

The chemical structure of chitin contains C-H, N-H and O-H and C = O bonds (Fig. 5), and the absorption peaks of chitin were retrieved from Roberts et al. [24], which was the 2nd derivative spectrum of D-glucosamine-HCl powder, a fungal cell wall polymer of glucosamine, and was scanned using an FT-NIR spectrometer by Roberts et al. [24]. The retrieved peaks were at 1195, 1505, 1583, 1733, 2110, 2265 (highest peak), 2308, 2368 and 2445 nm, where the higher absorption peaks were in the range of 2110–2455 nm and the 2nd highest peak range was between 1195 nm and 1505–1800 nm. These peaks were interpreted using the guidelines described by Osborne et al. [25]. The bands related to our study wavelength ranges were 1195, 1505 and 1583 nm.

With the same rationale for the explanation of the water bands, Table 2 shows the chitin bands, which are major components of the fungal cell wall; the 1195 nm band was the most important band, with the greatest difference in NIR absorption between the control and infected samples compared to the absorption of chitin at 1505 and 1583 nm.

In terms of the highest difference in absorbance during mango ripening at 8 days, the bands at 868, 1134, 1320 and 1069 nm differed more strongly (Table 3), indicating the effects of protein on cell wall vibration; vibration of the sugar and starch of the mango substrate; vibration of the NIR absorbers in the fungus-sprayed and mango substrate; and vibration of the crystallinity and N-acetyl methyl group in the fungal chitin and the constituents of the mango substrate, including water, sugar content, lipids, proteins, and methylated polysaccharides.

Table 1 Differences in the average 10 control (90 spectra) and 19 infected (323 spectra) sample absorbance values corresponding to the water bands

Wavelength (nm) (Experiment)			Reference wavelength (nm)	Bond vibration (Weyer and Lo, [21]; Kessler and Kessler, [22])	Difference in the absorbance of control and infected samples corresponding to water bands		
965.18	968.42	971.67	970	Combination, 2v1 + v3	0.0045066	0.0045195	0.0045275
1186.27	**1189.52**	**1192.78**	**1190, 1200**	**Combination, v1 + v2 + v3**	**0.0049115**	**0.0049013**	**0.0049154**
1446.92	1450.18	1453.44	1450	Combination, v1 + v3	0.0015018	0.0015049	0.0015071

v1 is the symmetric stretch, v2 is the bending mode, and v3 is the asymmetric stretch

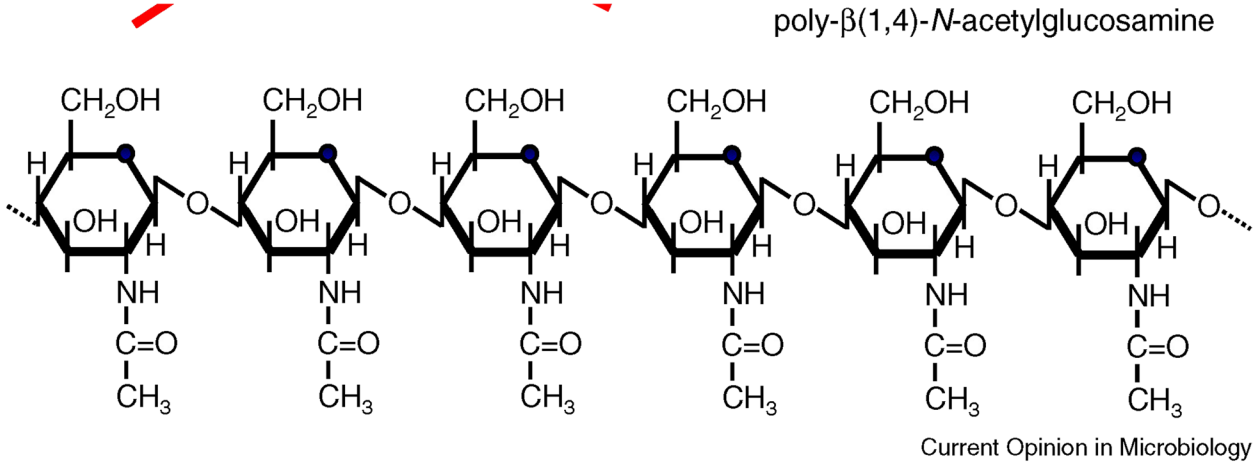

Fig. 5 Chemical structure of chitin [23]

Table 2 Differences in the average control (10 fruits with 90 spectra) and average infected (19 fruits with 323 spectra) sample absorbance values corresponding to the chitin bands

Wavelength (nm) (Experiment)	Reference wavelength (nm)	Bond vibration (Workman and Weyer [26]	Difference in the absorbance of the control and infected samples corresponding to chitin bands
1196.03	**1195**	**C-H (3v)**	**0.0049344**
1505.65	1505	N-H (2v)	0.0019642
1584.00	1583	O-H (2v)	0.0027838

2v is the 1 st overtone of the fundamental vibration and 3v is the 2nd overtone of the fundamental stretching bond vibration

Table 3 Maximum difference in the average absorbance between the original wavelength of control (10fruits with 90 spectra) and infected (19 fruits with 323 spectra) mango samples scanned on consecutive days for 8 days

DAY of Scanning	Sample number	Wavelength (nm) (Experiment)	Reference wavelength (nm)	Bond vibration	Maximum difference in absorbance
DAY 00	**19**	**864.53**	**868**	**Protein^**	**0.0069833**
DAY 01	19	864.53	868	Protein^	0.0045402
DAY 02	**19**	**1134.21**	**1134**	**No mention in ^^ and ^**	**0.0073413**
DAY 03	19	1316.52	1317		0.0045062
DAY 04	**19**	**1319.78**	**1320**		**0.0063698**
DAY 05	19	1326.29	1326		0.0044742
DAY 06	19	1329.55	1330		0.0029351
DAY 07	**19**	**1069.17**	**1069**	**2v O-H + δ C-H methyl ^^**	**0.0069121**

2v is the 1 st overtone of the fundamental stretching bond vibration stretching band, and δ is the fundamental bending bond vibration

^ Williams et al. [19]

^^Workman and Weyer [25]

The different absorbance intensities of noninfected and infected mangoes were compared between the specific NIR absorber bands, i.e., 3 water bands and 3 chitin bands (Tables 1 and 2, respectively), and 8 different days (Table 3); the difference in the mean was not statistically compared because the different NIR bands differed. This work aimed to specify the characteristics, especially the strength of the vibration, related to and affected by mango anthracnose, of specific bands and to propose bands for spectroscopic modelling.

Table 3 shows the maximum difference in absorbance between the original wavelength of the control and infected mango samples scanned on consecutive days for 8 days, which clearly shows the fluctuation of the difference in absorption. However, at DAY 00 and DAY 01, the greatest difference between the control and infected spectra was due to differences in protein absorption caused by the fungus sprayed on the infected mango. The maximum difference was observed with 1069 nm, which was the combination of 2ν O-H and δ C-H methyl, on DAY 07. 2ν O-H reflects H-bonding and crystallinity in chitin and indicates the water content, sugar content, ripeness, and spoilage of mango, and δ C-H methyl is vibrated by the N-acetyl methyl group in fungal chitin and by lipids, proteins, and methylated polysaccharides in the mango substrate [27]. However, for DAY 02–DAY 06, Williams et al. [20] and Workman and Weyer [26] did not show the vibration mode of these bands (1134, 1317, 1320, 1326, and 1330 nm). Therefore, an in-depth analysis of the related NIR bands to chitin in the cell wall of the fungus on mango peel was needed, and an analysis generated by ChatGPT [27] is presented in Table 4.

Chitin is a structural polysaccharide made of N-acetylglucosamine (GlcNAc) units (Fig. 2) and contains C–H (sugar backbone), N–H (acetamide groups), C = O (amide carbonyl) and O–H (hydroxyl groups in GlcNAc rings). In the NIR region (800–2500 nm; 12500–4000 cm^{-1}), the 1st overtone band can typically be estimated by (2×fundamental vibration wavenumber bands), the 2nd overtone by (3×fundamental wavenumber bands) and the combination of bands by (sum of two or more vibrations). Fundamental vibration occurred when the sample was subjected to mid-infrared (MIR) radiation. In Table 4, the NIR bands for the O-H, C-H, and N-H bond stretching modes are shown, where the energy of the bond bending mode was lower than that of the stretching mode; thus, it appeared at lower wavenumbers (longer wavelengths), which were in the MIR region. Although the fundamental O–H bending vibration (δ O–H) in mango tissue occurs at approximately 1640 cm^{-1} (6100 nm) in the mid-infrared region, it appears in the near-infrared primarily as a combination band (ν O–H + δ O–H) at approximately 1900–1950 nm, which is strongly associated with water and hydrogen-bonded polysaccharides. But spectrum range in this work is 800-1700 nm. The composition of mango fruits, which is related to NIR-active functional groups, is as follows: water → O–H stretching, sugars and starch → C–H, O–H combination, organic acids → C = O and O–H, proteins (minor) → N–H, carotenoids → C–H aromatic/aliphatic and fibre/cellulose → C–H and O–H bonds. These findings (Table 3 DAY 00) confirm that protein absorption by chitin differs between control and infected mangoes. The peak at 1134 nm, which resulted in the greatest difference in absorption between the control and infected mangoes at DAY 02 by the 2nd overtone of the C–H stretch of sugars and starch (Table 3), was the main component. These sugars and starch were related to the ripeness of the mangoes. In consideration of the vibration of the chitin in this band by the sugar-like structures (GlcNAc) in the chitin, the vibration of the sugar and starch of the mango was stronger. This difference in absorption was the greatest among the scanning days (DAY 00 to DAY 07). The 1333-1923 nm range involves O–H overtone and combination, strongly associated with moisture content and acid levels in mangoes, which are the mango maturity indicators. In the case of chitin, the 1333-1923 nm band involves O–H (1583 nm, Table 2) and N-H (1505 nm, Table 2) overtones and a strong chitin signal is detected for the hydroxyl and amide groups. Therefore, 1333-1923 nm bands combined the effects of both the mango substrate and the fungus.

Changes in the NIR spectrum corresponded to the infection mechanism of anthracnose growth

In our study, lesions caused by *C. asianum* anthracnose were observed at 168 h or 7 days after exposure at wavelengths ranging from 800 to 1700 nm. Anthracnose disease in mango is caused by a series of sequential

Table 4 The response of O-H, C-H, and N-H bond stretching modes to NIR and MIR radiation [26]

Bond Stretching Mode	Fundamental (cm^{-1})	Fundamental (nm)	1st Overtone (cm^{-1})	1st Overtone (nm)	Combination Bands (cm^{-1})	Combination Bands (nm)
O–H	~ 3400	~ 2941	~ 6800	~ 1471	5200–7500	~ 1923–1333
N–H	~ 3300	~ 3030	~ 6600	~ 1515	5200–7200	~ 1923–1389
C–H (sp^3)[#]	~ 2900	~ 3448	~ 5800	~ 1724	5500–8500	~ 1818–1176
C–H (aromatic)	~ 3030	~ 3300	~ 6060	~ 1650	~ 7500–8500	~ 1333–1176

[#]Chitin (GlcNAc units) where carbon atoms in the sugar ring mostly come from sp^3 hybridized carbon

processes, including conidial germination, melanized appressoria formation, penetration of the mango epidermis, and colonization of mango tissue when the spots start to appear. Specifically, conidia deposited on the surface of ripe mangos germinated after 12 h, appressoria developed during 14–96 h, and anthracnose symptoms started appearing at 5 days [28, 29]. The results indicated that the loss of water around the infected areas might be related to the structure of melanin compounds and the vibration of the N–H bond during the formation of appressoria of the fungus *Colletotrichum* [30]. The skin of mango fruits was damaged only by anthracnose pathogens [31]. The range of time in Fig. 5 was from DAY 00 to DAY 03, in which absolutely no appearance of anthracnose on mango was detected.

The average spectra of control and infected mangoes of cv. Namdokmai Sithong shown in Fig. 6(A) and those shown in Fig. 6(B) for mangoes pretreated via standard normal variate show the water peaks [974 (shifted peak from 970 nm), 1190, 1450 and 1583 nm]. The anthracnose growth of the infected mangoes corresponded to changes in the NIR spectrum at 4 days after the spore was deposited, as discussed below.

The vibration bands of the liquid water at room temperature were 970 and 1450 nm; although these two bands are generally referred to as the 2nd and 1st overtones of the O-H stretch, they were actually combined bands of 2ν1 + ν3 and ν1 + ν3, respectively, the weak broad peak at 1190 nm is ν1 + ν2 + ν3 [25], and 1450 nm is also the band of starch [25]. As mentioned, 1583 nm is the O-H stretching and O-H bending combination band of water [26].

These results are in accordance with those of Sirisomboon et al. [32], who confirmed that the moisture and starch content in rice affects the overall extent of fungal infection. The moisture content of the substrate is among the most important factors governing fungal growth and mycotoxin production [33].

As shown in Fig. 6(B), the SNV spectra in the zoom mode of the peaks at 974 and 1450 nm revealed higher absorption in anthracnose-infected mangoes than in noninfected mangoes, indicating that the NIR absorption vibration is greater in water and starch. The absorption of the infected mangoes decreased at 1450 nm from DAY 00 to DAY 03 (0–96 h, when appressoria developed) compared with that at 974 nm, indicating that the effect of the combination of starch and water is stronger than that of water alone. This does not contradict our result in Table 1 for the greatest difference in absorbance between the noninfected and infected mangoes at 1190 nm, which is the combination of symmetric stretching, bending and asymmetric stretching of O-H bonds, which is different from the vibration at 970 nm for the combination of 2 of symmetric stretching and asymmetric stretching of O-H bonds. The fluctuation in water absorption at 974 nm might be due to the diffusion of NIR radiation in the deeper layer of the fruit due to the higher photon energy faced by the greater variation in the peel and pulp matrix. The growth of the appressoria resulted in the consumption of increasing amounts of water and starch in the mango substrate for 14–96 h, as indicated by a decrease in absorption at 1450 nm (Figure 6(B)). Noninfected and infected mangoes were kept in a closed transparent plastic box, which revealed that the change in the water content in the top layer of the mango fruits at 1190 nm increased from DAY 00 to DAY 03 because the increasing respiration of mango during storage caused the air–water mixture to provide a lower air: water ratio, causing the water to evaporate to the environment in the box. At 1190 nm, the water content of the infected mangoes increased from DAY 00 to DAY 03 but was less than the water content of the control mangoes, indicating that more water was consumed by the fungus-infected mango than by the mango with no fungus. This finding confirms the high possibility of a 1190 nm absorption band for differentiating noninfected and infected mangoes and early detection. Simultaneously, the increase in the chitin vibration at the nearby band at 1195 nm from DAY 00 to DAY 03 confirmed fungal cell wall growth during storage. The absorption bands of chitin at 1505 and 1573 nm were not peaks because the abundance of the broad water and starch band was much greater than that of the fungus in this stage.

Benefit of the deposition method for fungal spores spread throughout the mango fruit surface

The method of depositing fungal spores involves spraying the spores throughout the mango fruit surface, not on a small area or at a specific point. It can be used to not only vary the concentration of spores but also quantify the number of spores per unit area exactly. The hyperspectral imaging camera can be harmonized using only the proposed method, where every pixel of a mango image can be detected even with different numbers of spores distributed on the surface concurrent with the occurrence of anthracnose on fruits such as mango (Fig. 1). It is suitable for practical detection situations. Thus far, no applications have been used for mango anthracnose research.

Conclusions

Three (3) aspects of the experiment can be concluded upon: (1) the method of natural simulation to deposit the fungal spores all over the mango surface by spraying the spore suspension onto the surface, where the conidia penetrate unaided beneath the mango peel, (2) the important wavelengths for differentiating the control (noninfected) and anthracnose fungus-infected mangoes by using different absorbances on the NIR spectra

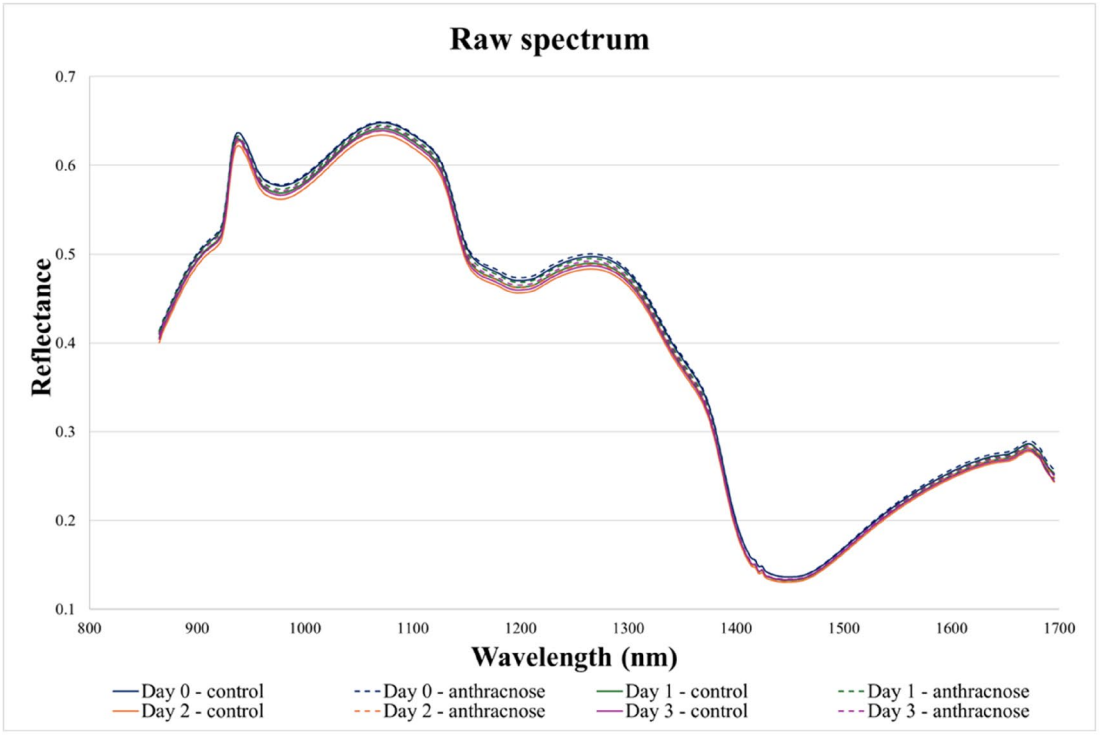

A

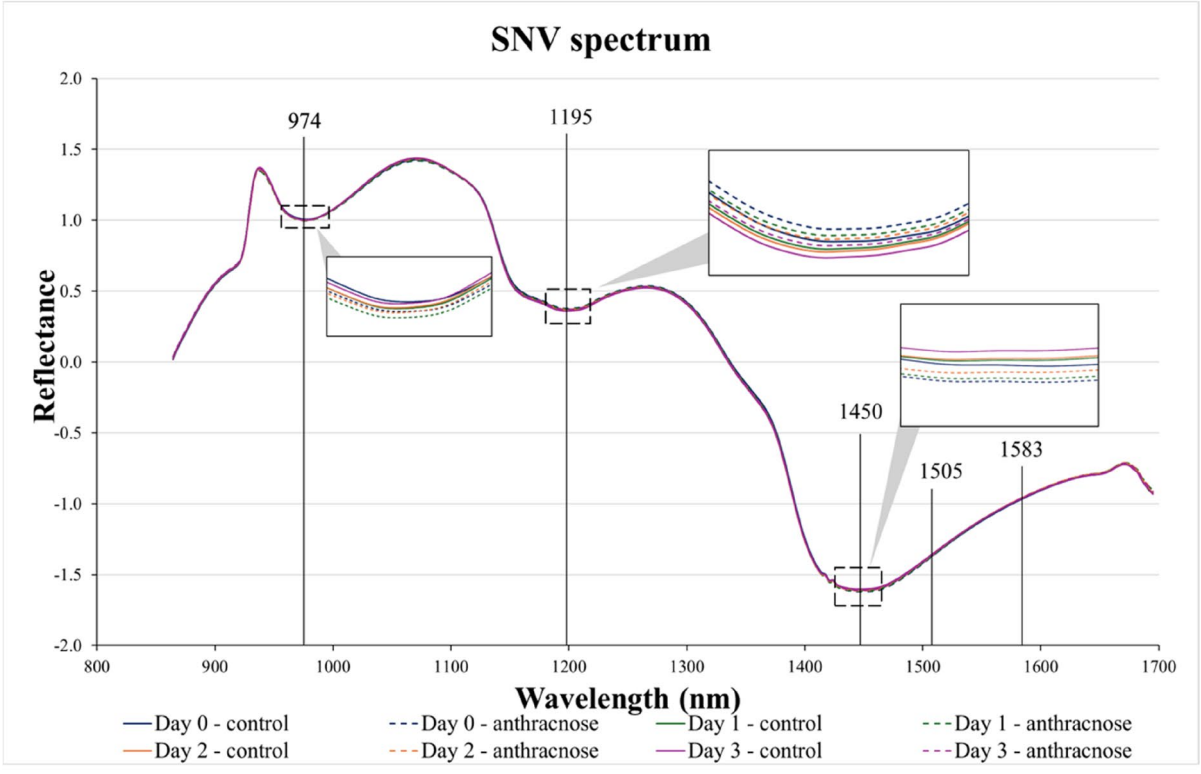

B

Fig. 6 Spectra of mangoes of cv. Namdokmai Sithong: **A** average and **B** pretreated with standard normal variate

of both groups, and (3) the microbiological mechanism of anthracnose growth on the infected mangoes corresponding to changes in the NIR spectrum at 4 days after the infection of the pathogen.

The proposed method of depositing fungal spores by spraying the spores throughout the mango fruit surface, not within a small area or specific point, can facilitate the use of a hyperspectral imaging camera in conjunction with chemometric modelling to detect different numbers of spores, which is suitable for practical detection situations.

The important wavelengths for differentiating the control (noninfected) and anthracnose fungus-infected mangoes by using different absorbances on the NIR spectra of both groups obtained in our study were the water bands at 970 and 1190 or 1200 nm and the chitin band at 1195 nm. In terms of the greatest difference in absorbance during mango ripening (8 days), the bands at 868, 1134, 1320 and 1069 nm differed from each other, indicating the effects of the vibration of crystalline compounds and N-acetyl methyl groups on fungal chitin, water, starch, protein, sugar, lipids, and methylated polysaccharides.

The change in the NIR spectra during the 4 days of anthracnose growth on the infected mangoes corresponds to the microbiological mechanism of appressoria growth and mango ripening. The peaks at 1450 and 1190 nm indicated that the NIR absorption vibration was due to water and starch consumed for appressorium growth. Moreover, the chitin vibration at the band near 1195 nm, which was reconfirmed to be the most important among the NIR bands of chitin, was determined by spectral observation of increased fungal cell wall growth.

These results can be beneficial for differentiating nonlesioned anthracnose-infected mangoes from non-infected ones using an NIR-HSI sensor. The important wavelengths related to the growth of anthracnose in mango peel can be applied to enhance early detection or normal evaluation by quantitative and qualitative techniques using online NIR-HSI for the whole fruit of mango in the mango export industry.

Abbreviations

C	Carbon
CFU	Colony-forming units
C–H	Carbon–Hydrogen bond
C=O	Carbonyl bond
FT-NIR	Fourier transform near-infrared
GlcNAc	N-acetylglucosamine
H	Hydrogen
N	Nitrogen
N-acetylglucosamine	Nitrogen-acetylglucosamine
N–H	Nitrogen–Hydrogen bond
O	Oxygen
O-H	Hydroxyl bond
MIR	Mid-infrared
nm	Nanometre
NIR	Near infrared
NIR-HSI	Near-infrared hyperspectral imaging
NIRS	Near-infrared spectroscopy
PLS-DA	Partial least squares discriminant analysis
RGB	Red, Green, Blue
UV-C	Ultraviolet radiation with a wavelength range of 100 to 280 nanometres
Vitamin C	A water-soluble vitamin, also known as ascorbic acid
Vitamin E	A fat-soluble vitamin
QDA	Quadratic discriminant analysis
sp^3	A type of bonding in which one s orbital and three p orbitals of an atom mix to form four equivalent sp^3 hybrid orbitals
spp.	Species
2ν	1^{st} overtone of the fundamental stretching bond vibration
3ν	2^{nd} overtone of the fundamental stretching bond vibration
δ	Fundamental bending bond vibration absorption band

Acknowledgements
The authors express their deep gratitude to Assoc. Prof. Dr. Somsiri Sangchote of Kasetsart University, Thailand, for his invaluable recommendation on a practical method for quantifying fungal spores. The authors would like to thank the Near-Infrared Hyperspectral Image Laboratory in the Department of Agricultural Engineering, Faculty of Engineering Kampangsang, Kasetsart University, Kampangsan campus, Thailand, for the use of a hyperspectral imager and space for experiments and the Laboratory of Microbiology in the Faculty of Science, Chulalongkorn University, Thailand, for microbiology sample preparation. We thank the Thailand Science Research and Innovation (TSRI) and King Mongkut's Institute of Technology Ladkrabang for the Fundamental Fund for the fiscal year 2023, Grant number RE-KRIS/FF66/42 and the School of Engineering, King Mongkut's Institute of Technology Ladkrabang for the grant to an assistant researcher, contract number 2566-02-01-044.

Authors' contributions
All the authors contributed to the study conception and design. Material preparation, data collection and analysis were performed by Apiwat Junto and Thitima Phanomsophon. The first draft of the manuscript was written by Apiwat Junto, Cheewanun Dachoupakan Sirisomboon, Panan Rerngsamran and Panmanas Sirisomboon, and all the authors commented on previous versions of the manuscript. All the authors read and approved the final manuscript.

Funding
This work was supported by the Thailand Science Research and Innovation (TSRI) and King Mongkut's Institute of Technology Ladkrabang for Fundamental Fund for the fiscal year 2023 [Grant number RE-KRIS/FF66/42] and the School of Engineering, King Mongkut's Institute of Technology Ladkrabang for the grant to an assistant researcher [Contract number 2566-02-01-044].

Data availability
The datasets and materials generated during and/or analysed during the current study are available from the corresponding author upon reasonable request.

Declarations

Ethics approval and consent to participate
Not applicable, as this study did not include human or animal research.

Consent for publication
Not applicable.

Competing interests
The authors declare no competing interests.

Author details
[1]School of Engineering and Innovation, Rajamangala University of Technology, Tawan-ok, Chonburi 20110, Thailand

[2]Office of Administrative Interdisciplinary Program on Agricultural Technology, School of Agricultural Technology, King Mongkut's Institute of Technology Ladkrabang, Bangkok, Thailand
[3]Department of Primary Industries and Regional Development, Perth, WA 6000, Australia
[4]Department of Agricultural Engineering, School of Engineering, King Mongkut's Institute of Technology Ladkrabang, Bangkok 10520, Thailand
[5]Department of Microbiology, Faculty of Science, Chulalongkorn University, Bangkok 10330, Thailand
[6]Department of Food Engineering, School of Engineering, King Mongkut's Institute of Technology Ladkrabang, Bangkok, Thailand
[7]Department of Biological and Agricultural Engineering, Faculty of Engineering, Universiti Putra Malaysia, Serdang, Selangor 43400, Malaysia
[8]SMART Farming Technology Research Centre (SFTRC), Faculty of Engineering, Universiti Putra Malaysia, Serdang, Selangor 43400, Malaysia
[9]Department of Computer Engineering, Chulalongkorn University, Bangkok 10330, Thailand
[10]Department of Agricultural Engineering, Faculty of Engineering at Kamphaeng Saen, Kasetsart University, Kamphaeng Saen, Nakhon Pathom 73140, Thailand

Received: 17 July 2025 / Accepted: 24 November 2025
Published online: 16 December 2025

References

1. Rattanakreetakul C, Keawmanee P, Bincader S, Mongkolporn O, Phuntumart V, Chiba S, Pongpisutta R. Two newly identified *Colletotrichum* species associated with Mango anthracnose in central Thailand. Plants. 2023;12(5):1130. https://doi.org/10.3390/plants12051130.
2. Ntsoane ML, Zude-Sasse M, Mahajan P, Sivakumar D. Quality assessment and postharvest technology of mango: a review of its current status and future perspectives. Sci Hortic (Amsterdam). 2019;249:77–85. https://doi.org/10.1016/j.scienta.2019.01.033.
3. TPSO. (2024) Thai Mango, a rising star in fruit exports, South Korea rises to No. 1 in Thailand's export market. Trade policy and strategic office, Ministry of Commerce, Thailand. https://tpso.go.th/news/2502-0000000040.
4. Dofuor AK, Quartey NKA, Osabutey AF, Antwi-Agyakwa AK, Asante K, Boateng BO, Ablormeti FK, Lutuf H, Osei-Owusu J, Osei JHN, Ekloh W. Mango anthracnose disease: the current situation and direction for future research. Front Microbiol. 2023;14:1168203. https://doi.org/10.3389/fmicb.2023.1168203.
5. Uddin M, Shefat S, Afroz M, Moon N. Management of anthracnose disease of Mango caused by *Colletotrichum gloeosporioides*: A review. Acta Sci Agric. 2018;2:169–77. https://www.researchgate.net/publication/329519803.
6. Matulaprungsan B, Wongs-Aree C, Penchaiya P, Boonyaritthongchai P, Srisurapanon V, Kanlayanarat S. Analysis of critical control points of post-harvest diseases in the material flow of Nam dok Mai Mango exported to Japan. Agric. 2019;9(9):200. https://doi.org/10.3390/agriculture9090200.
7. Tangpao T, Phuangsaujai N, Kittiwachana S, George DR, Krutmuang P, Chuttong B, Sommano SR. Evaluation of markers associated with physiological and biochemical traits during storage of 'Nam dok Mai Si thong' Mango fruits. Agriculture. 2022;12:1407. https://doi.org/10.3390/agriculture12091407.
8. Danh LT, Giao BT, Duong CT, Nga NTT, Tien DTK, Tuan NT, Huong BTC, Nhan TC, Trang DTX. Use of essential oils for the control of anthracnose disease caused by *Colletotrichum acutatum* on post-harvest mangoes of Cat Hoa Loc variety. Membranes. 2021;11:719. https://doi.org/10.3390/membranes11090719.
9. Abd-Alla MA, Haggag WM. Use of some plant essential oils as post-harvest botanical fungicides in the management of anthracnose disease of Mango fruits (*Mangifera indica* L.) caused by *Colletotrichum gloeosporioides*. Int J Agric Sci for. 2013;3(1):1–6. https://doi.org/10.5923/j.ijaf.20130301.01. Penz.
10. Sripong K, Jitareerat P, Tsuyumu S, Uthairatanakij A, Srilaong V, Wongs-Aree C, Ma G, Zhang L, Kato M. Combined treatment with hot water and UV-C elicits disease resistance against anthracnose and improves the quality of harvested mangoes. Crop Prot. 2015;77:1–8. https://doi.org/10.1016/j.cropro.2015.07.004.
11. Manley M. Near-infrared spectroscopy and hyperspectral imaging: Non-destructive analysis of biological materials. Chem Soc Rev. 2014;43(24):8200–14. https://doi.org/10.1039/C4CS00062E.
12. Fazari A, Pellicer-Valero OJ, Gómez-Sanchıs J, Bernardi B, Cubero S, Benalia S, Zimbalatti G, Blasco J. Application of deep convolutional neural networks for the detection of anthracnose in olives using VIS/NIR hyperspectral images. Comput Electron Agric. 2021;187:106252. https://doi.org/10.1016/j.compag.2021.106252.
13. Velásquez C, Prieto F, Palou L, Cubero S, Blasco J, Aleixos N. New model for the automatic detection of anthracnose in Mango fruits based on Vis/NIR hyperspectral imaging and discriminant analysis. J Food Meas Charact. 2024;18(1):560–70. https://doi.org/10.1007/s11694-023-02173-3.
14. Sonthiya K, Seehanam P, Theanjumpol P, Maniwara P. Detection of anthracnose disease in 'Namdokmai sithong' Mango using near infrared spectroscopy. J Agric. 2022;38(2):237–48. (in Thai). https://li01.tci-thaijo.org/index.php/joacmu/article/view/253107.
15. National Bureau of Agricultural Commodity and Food Standards. (2024) Thailand Agricultural Standard: (TAS 5-2024) Mango (in Thai) https://acfs-backend.acfs.go.th/storage/ProductStandards/Files//20241111142055_324736.pdf (write the date of access the literature).
16. Penchaiya P, Tijskens LMM, Uthairatanakij A, Srilaong V, Tansakul A, Kanlayanarat S. Modelling quality and maturity of 'Namdokmai sithong' Mango and their variation during storage. Postharvest Biol Technol. 2020;159:111000. https://doi.org/10.1016/j.postharvbio.2019.111000.
17. Zhang K, Su Y-Y, Lei C. An optimized protocol of single spore isolation for fungi. Cryptogam Mycol. 2013;34(4):349–56. https://doi.org/10.7872/crym.v34.iss4.2013.349.
18. Khalil HA, Abdelkader MFM, Lo'ay AA, El-Ansary DO, Shaaban FKM, Osman SO, Shenawy IE, Osman H-EH, Limam SA, Abdein MA, Abdelgawad ZA. The combined effect of hot water treatment and Chitosan coating on Mango (*Mangifera indica* L. cv. Kent) fruits to control postharvest deterioration and increase fruit quality. Coatings. 2022;12(1):83. https://doi.org/10.3390/coatings12010083.
19. Tsai C-M, Guan S-S. Identifying regions of interest in reading an image. Displays. 2015;39:33–41.
20. Williams P, Manley M, Antoniszyn J. Near-infrared technology: getting the best out of light. South Africa. 301 pp: SUN; 2019.
21. Weyer LG, Lo SC. Spectra-structure correlations in the near-infrared. In: Chalmers JM, Griffiths PR, editors. Handbook of vibrational spectroscopy. Chichester, UK: John Wiley & Sons, Ltd.; 2006; Volume 3, pp. 1817–1837. https://doi.org/10.1002/9780470027325.s4102.
22. Kessler RW, Kessler W. Inline and online process analytical technology with an outlook for the petrochemical industry. In: Ozaki Y, Huck C, Tsuchikawa S, Engelsen SB, editors. Near-infrared spectroscopy. Singapore: Springer; 2021. 586 pp https://doi.org/10.1007/978-981-15-8648-4_23.
23. Lenardon MD, Munro CA, Gow NA. Chitin synthesis and fungal pathogenesis. Curr Opin Microbiol. 2010;13(4):416–23. https://doi.org/10.1016/j.mib.2010.05.002.
24. Roberts CA, Moore KJ, Graffis DW, Kirby HW, Walgenbach RP. Quantification of mold in hay by near infrared reflectance spectroscopy. J Dairy Sci. 1987;70:2560–4. https://doi.org/10.3168/jds.S0022-0302(87)80324-7.
25. Osborne BG, Fearn T, Hindle PT. Practical NIR spectroscopy with applications in food and beverage analysis. Longman group, UK. 1993. https://a.co/d/iOhM1JH.
26. Workman J Jr, Weyer L. Practical guide to interpretive near-infrared spectroscopy. Boca Raton: CRC; 2007. https://doi.org/10.1201/9781420018318.
27. OpenAI. (2025) ChatGPT (June 2 version) [Large language model].
28. Dinh S-Q, Chongwungse J, Pongam P, Sangchote S. Fruit infection by *Colletotrichum gloeosporioides* and anthracnose resistance of some Mango cultivars in Thailand. Australas Plant Pathol. 2003;32:533–8. https://doi.org/10.1071/AP03053.
29. Ganesan S, Kumari N, Sahu S, Pattanaik M, Raj A, Panda M, Srinivas P, Singh HS. Characterization of *Colletotrichum* species causing new pre-harvest anthracnose symptoms on Mango in Eastern India. Australas Plant Pathol. 2024;53:239–52. https://doi.org/10.1007/s13313-024-00973-9.
30. Kubo Y, Suzuki K, Furusawa I, Yamamoto M. Melanin biosynthesis as a prerequisite for penetration by appressoria of *Colletotrichum lagenarium*: site of Inhibition by melanin inhibiting fungicides and their action on appressoria. Pestic Biochem Physiol. 1985;23(1):47–55. https://doi.org/10.1016/0048-3575(85)90077-X.
31. Jenny F, Sultana N, Islam MM, Khandaker MM, Bhuiyan MAB. A review on anthracnose of Mango caused *Colletrotrichum gloeosporioides*. Bangladesh J Plant Pathol. 2019;35:65–74. https://bps.net.bd/wp-content/uploads/2020/12/10.-A-REVIEW-ON-ANTHRACNOSE-OF-MANGO-CAUSED-BY-COLLETOTRICHUM-GLOEOSPORIOIDES.pdf.

32. Sirisomboon CD, Putthang R, Sirisomboon P. Application of near infrared spectroscopy to detect aflatoxigenic fungal contamination in rice. Food Control. 2013;33:207–14. https://doi.org/10.1016/j.foodcont.2013.02.034.
33. Pitt JI, Hocking AD. Fungi and food spoilage. 3rd, Springer, New York. 2009. https://doi.org/10.1007/978-0-387-92207-2.

Publisher's Note